J. Mod. Transport. (2013) 21(2):103–110
DOI 10.1007/s40534-013-0012-0

www.springer.com/40534

Numerical determination for optimal location of sub-track asphalt layer in high-speed rails

Mingjing Fang · Sergio Fernández Cerdas · Yanjun Qiu

Received: 22 February 2013 / Revised: 18 March 2013 / Accepted: 29 March 2013 / Published online: 20 June 2013

Abstract Well-graded asphalt mix with the merits of high sound absorption, low water permeability, excellent strength, and easy construction is an important option for high-speed railway substructures. On the basis of finite element method, a model with conventional ballasted trackbed (T_0) and four ballasted trackbeds models with different positions of asphalt layer were analyzed, in which 15 cm thick asphalt layer was used to replace the different sub-track layers, the bottom and the top of upper subgrade and of ballasted trackbed, named as T_1, T_2, T_3, and T_4, respectively. The results showed that the range of peak vertical accelerations on the top of subgrade surface of T_2 and T_4 were smaller than T_1 and T_3; T_1 and T_2 perform better in decreasing the maximum vertical deformation of subgrade than T_3 and T_4; the maximum transversal tensile strain of T_4 is almost twice than the other three. The trackbed bears more stress when the asphalt layer is located at the lower part of railway trackbed.

M. Fang (✉)
Department of Road & Bridge Engineering, School of Transportation, Wuhan University of Technology, Wuhan 430063, Hubei, People's Republic of China
e-mail: mingjingfang@whut.edu.cn

S. F. Cerdas
Costa Rica Institute of Technology, Construction Engineering School, Cartago 159-7050, Costa Rica
e-mail: sefernandez@itcr.ac.cr

Y. Qiu
Key Lab of Highway Engineering of Sichuan Province, Southwest Jiaotong University, Chengdu 610031, People's Republic of China
e-mail: yjqiu@home.swjtu.edu.cn

Keywords High-speed railways · Asphalt concrete · Ballasted trackbed · FEM · Numerical analysis

1 Introduction

The conventional ballasted trackbed is still an important option for high-speed railway substructures due to its good performance for vibration control and noise reduction as well as low cost and easy construction. To meet the requirements of high-speed trains, conventional ballasted trackbeds need to be more enhanced to prevent the subgrade deterioration. Well-graded asphalt concrete has capability for this enhancement due to its low permeability, sufficient strength, and appropriate flexibility as well as easy construction and quick maintenance.

Asphalt trackbeds have already been used internationally with great acceptance, while the asphalt layer in railway substructures is not placed in the same position. Momoya [1, 2] introduced a new performance-based design method and considered the effects of the number of passing trains on the fatigue of asphalt mixture layer. Teixeira et al. [3] presented bituminous track design and found that structural performance was good when a 12-cm to 14-cm conventional bituminous subballast layer was used in lieu of the usual granular layers. In Italy, more than 1,200 km high-speed lines have been equipped with asphalt sub-ballast layer since 1970s [3]. Huurman et al. [4] investigated the possibilities of embedded rail in asphalt (ERIA) and used cement-filled, porous asphalt as the bitumen-bound alternative for cement-bound concrete. In US, two methods have been used to incorporate hot mix asphalt (HMA) in railroad trackbeds [5]. One method is to place the HMA on the top of subgrade and the ties directly on the asphalt mat, which is called overlayment. Another

method used more often is called underlayment referring to the asphalt mat placed under the ballast to serve as sub-ballast. A program KENTRACK was developed for the asphalt trackbed design [6]. In China, because the Portland Cement Concrete (PCC) has been the fundamental material in high-speed rails since the 1990s [7], very few related research were referred.

The main objective of this work is to determine the optimal location of asphalt layer paved in conventional trackbed via numerical analysis with finite element method (FEM) program ABAQUS®. During the modeling, 15 cm thick asphalt layer was used to replace the bottom and the top of upper subgrade and conventional ballasted trackbed T_0 respectively. Based on a comprehensive analysis of key mechanical parameters such as the vertical stresses at the top of subgrade and the transversal and longitudinal tensile strain at the bottom of asphalt layer, the optimal location of railway asphalt can be determined.

2 Dynamic FEM modeling theory and parameters

2.1 Dynamic FEM modeling theory

The motion equation of structure model for dynamic simulation is generally represented by second-order ordinary differential equations [8],

$$M\ddot{a}(t) + C\dot{a}(t) + Ka(t) = Q(t), \quad (1)$$

where, $\boldsymbol{M}$ is the mass matrix; $\boldsymbol{K}$ is the stiffness matrix; $\boldsymbol{C}$ is the structural damp matrix; $\boldsymbol{a}(t)$ is the node displacement vector; $\ddot{\boldsymbol{a}}(t)$ is the nodal acceleration vector; $\boldsymbol{Q}(t)$ represents all external force vectors.

By solving Eq. (1), the displacement vector $\boldsymbol{a}(t)$ could be derived. The stress $\sigma(t)$ and strain $\varepsilon(t)$ of each element can be derived from the relationship between displacement and stress or strain. Compared to static processing, the dynamic FEM analysis involves mass matrix and damp matrix because of the occurrence of kinetic energy and dissipation in energy equation, and the solution is not derived from algebraic equations but from ordinary differential equations.

2.2 Dynamic structural parameters

From above, the derivation of dynamic FEM solution requires to determine the mass matrix, damping matrix or stiffness matrix. As for the calculation of the mass matrix, the shape functions are the same with displacement interpolation function, damping matrix is the linear combination of mass matrix, and stiffness matrix can be calculated by $\boldsymbol{C} = \alpha\boldsymbol{M} + \beta\boldsymbol{K}$, where, both α, β are constants which are determined by the natural frequency and corresponding damping ratio. The circular frequency ω_1 and corresponding damping ratio ξ_1 are applied to obtain $\alpha = \xi_1\omega_1, \beta = \xi_1/\omega_1$. Different geometry features and boundary conditions can influence the damping coefficient of FEM models.

In the following numerical analysis, the Rayleigh damping function is used. First, the mass matrix $\boldsymbol{M}$ and stiffness matrix $\boldsymbol{K}$ are constructed with the known density and modules of structure model. Then, the natural frequencies of asphalt track models are extracted by the method of linear perturbation. Combining these frequencies with the given damping ratio, the Rayleigh damping coefficient of the corresponding trackbed model is calculated.

3 FEM modeling for railway asphalt ballasted trackbeds

3.1 Geometry features of railway substructure

The sub-track area influenced by dynamic train loads could be partitioned into four layers, the bottom and the top of the upper subgrade and of the trackbed. For these layers, the materials were replaced by 15 cm thick HMA respectively, and the corresponding models were named as T_1, T_2, T_3, and T_4. Figure 1 shows the geometric features of T_0 and four asphalt trackbed models by replacing different layer locations of T_0. In order to minimize the negative effect of the boundary condition, especially the reflected wave from boundary, the model T_0 has a 15 m length in the longitudinal direction and the calculation area is located in the middle of the model with the size of 5 m.

3.2 FEM modeling parameters

For simplification, the material has elastic properties. The calculations follow the provisional design specification [9]. The asphalt mix with the asphalt binder 70# has the nominal maximum size (NMS) 25 mm and the recommended gradation range is listed in Table 1 [10].

All parts in models were simulated by solid element. Spring/Dashpots were adopted to simulate the contact between rails and sleepers as shown in Fig. 2. The spring spacing is 0.6 m. The interlayer behaviors of trackbeds are not considered in the calculation.

Basically, the dynamic modulus of asphalt mixtures depends on the test temperature (strongly related) and load frequency, the mix type, the material properties and the test methods. Four dynamic modulus values, 5,760, 4,739, 4,620, and 3,870 MPa were gained from several tests at 25 °C [11]. The average value is 4,747 MPa. Bei [12] defined the average modulus in four seasons, spring, summer, fall, and winter, as 4,812, 2,562, 8,618, and 15,715 MPa, respectively.

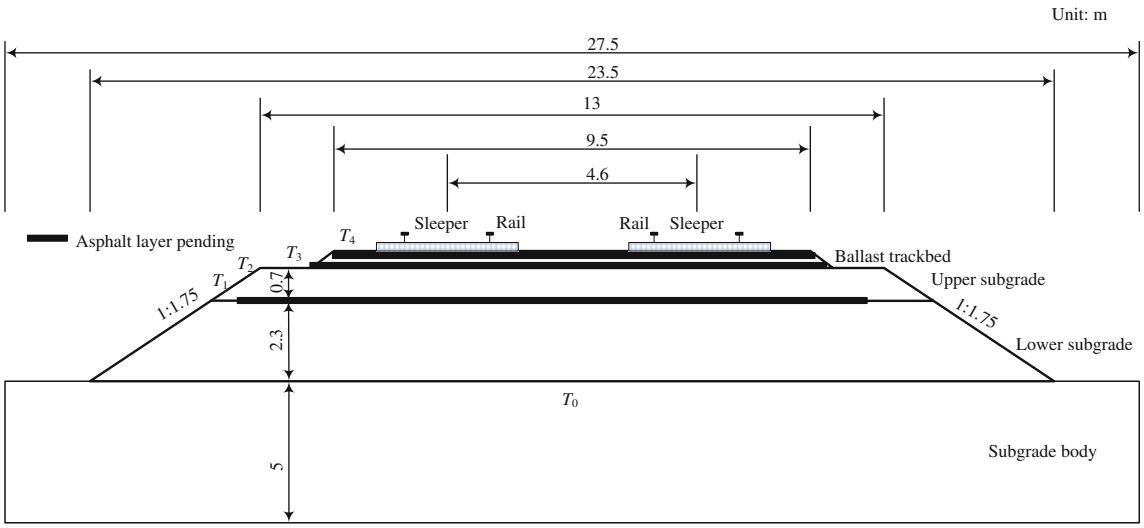

Fig. 1 Cross section of ballasted trackbed T_0 and four sub-track asphalt layers

Table 1 Gradation range of sub-track asphalt mix

Size/mm	Passing/%	Size/mm	Passing/%
37.5	100	2.36	19–45
26.5	90–100	1.18	14–34
19	78–95	0.6	10–25
16	67–87	0.3	5–17
13.2	56–80	0.15	3–10
9.5	42–68	0.075	1–7
4.75	29–57	<0.075	–

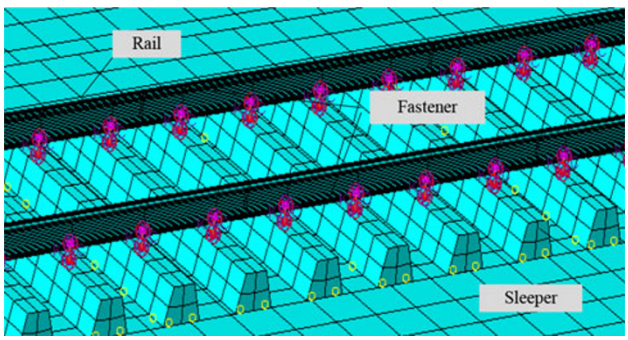

Fig. 2 Contact between rails and sleepers

The averaged value is 7,927 MPa. Here, 4,000 MPa was used as the reasonable modulus value of the asphalt mixture. In addition, the Poisson's ratio and density of asphalt mix were taken as 0.35 (25 °C) and 2,400 kg/m^3 [13]. The material parameters are listed as Tables 2 and 3. As for the contact and boundary conditions, the CAE module *Interaction* that defines the contact relationship was used between two adjacent parts. Meshing with C3D8R element worked appropriately due to its great precision to display the FEM analysis results. The model T_0 after meshing is shown in Fig. 3.

For the ease of analysis, the self-weight stress field was not considered in the analysis. The boundary constraints were applied with 6 DOFs (degree of freedoms), and the longitudinal and transversal directions has symmetric boundary conditions.

3.3 Train load simulation

As to super-long jointless tracks that have been widely used in high-speed railway lines, the main factor to influence the vertical behavior of trains is the ride performance. Therefore, we adopt the excitation load which is the superposition of static wheel load and dynamic load in the form of multiple sinusoidal functions to simulate train load. For simplification, the ellipse area of wheel-rail contact zone was replaced by rectangular area in the load modeling (see Fig. 4).

The simplified expression to describe dynamic train load is [14],

$$F(t) = P_0 + P_1 \sin \omega_1 t + P_2 \sin \omega_2 t + P_3 \sin \omega_3 t, \qquad (2)$$

Table 2 Material parameters for FEM modeling

Modeling parts	Density (kg/m^3)	Elasticity Modulus (Pa)	Poisson's Ratio	Stiffness damping ratio	Materials
Rail	7,830	2.06×10^{11}	0.30	0.015	Steel et al.
Sleeper	2,800	3.50×10^{10}	0.20	0.030	Reinforced cement concrete
Ballast	2,200	1.50×10^{8}	0.27	0.040	Crushed graded stone
Trackbed surface	2,150	1.20×10^{8}	0.30	0.059	Crushed graded stone
Trackbed bottom	1,900	0.70×10^{8}	0.30	0.031	A, B filler, modified soil
Subgrade body	1,800	0.50×10^{8}	0.34	0.035	A, B, C filler, modified soil

Table 3 Comprehensive evaluation to four asphalt railway trackbeds

Structural styles	Key parameters			
	Top of subgrade surface		Bottom of asphalt layer	
	Vertical acceleration	Vertical deformation	Transversal strain	Longitudinal strain
T_1	×	√	√	√
T_2	√	√	√	√
T_3	×	×	√	×
T_4	√	×	×	×

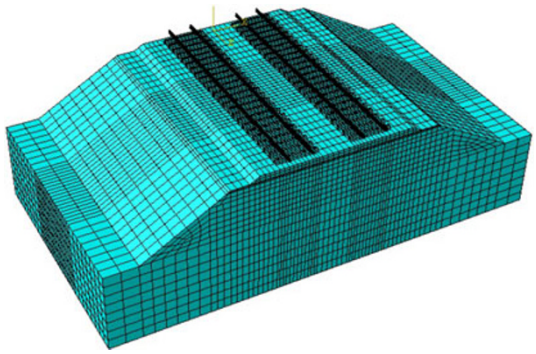

Fig. 3 FEM model T_0 after meshing

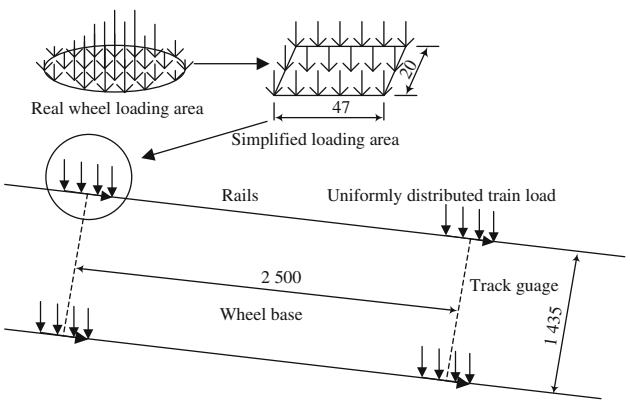

Fig. 4 Schematic of dynamic train load (unit: mm)

where, P_0 is static wheel load on one side; P_1, P_2, P_3 are vibration loads in three control conditions: train stationary (I), additional load (II), and corrugations effect (III); t stands for the time. If the unsprung weight is M_0, the amplitude of vibration load is,

$$P_1 = M_0 \alpha_i \omega^2, \tag{3a}$$

where, α_i and ω_i are the vector height and the circular frequency under the constraint three conditions I, II, III. ω_i is calculated by

$$\omega_i = 2\pi v / L_i, \tag{3b}$$

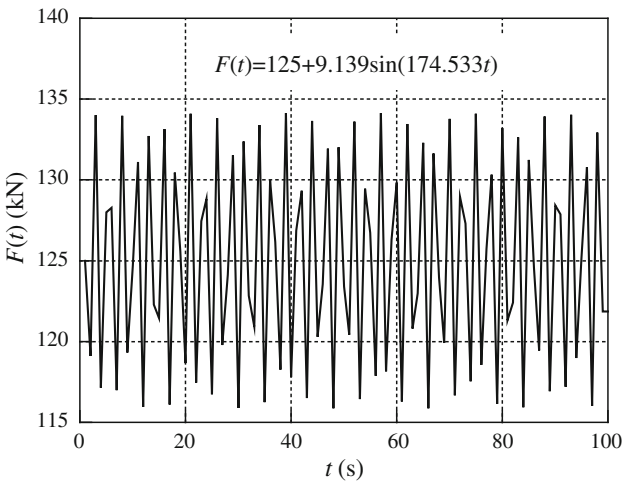

Fig. 5 Time-history curves of load (v = 200 km/h)

where, v denotes train speed, L_i denotes the wave length of vibration load under the three control conditions. Here, the dynamic additional load and corrugation effect are not the main focus. Thus, the train load is simplified as

$$F(t) = P_0 + P_1 \sin \omega t, \tag{4a}$$

$$P(t) = F(t)/A = (P_0 + P_1 \sin \omega t)/A, \tag{4b}$$

where A denotes wheel-rail contact area.

In the calculation, $P_0 = 125$ kN,$M_0 = 750$ kg, $\alpha = 0.4$ mm, $A = 940$ mm^2, $L = 2$ m. When $v = 200$ km/h [7], $\omega = 174.533$ Hz, and $P_1 = 9.139$ kN, the time-history curve of exciting force is shown in Fig. 5.

4 Calculation results and analysis

4.1 Validation of T_0 model

The time-history curves (scattered) of acceleration on the top subgrade of four asphalt trackbeds were compared with those of T_0 as shown in Fig. 6a–d.

The amplitude of maximum vertical acceleration of model T_0 is -25 to 40 m/s^2, but there are several peak values in the range of 10–20 m/s^2. This result is similar to the one in Ref. [15]. ranging from 14 to 16 m/s^2. The range of elastic deformation is 1.0–2.3 mm, which is close to 1.2–2.3 mm obtained by Su and Cai [16]. The peak value of vertical stress on subgrade surface is about 50 kPa, which is in the range of 41–57 kPa measured from field tests [17]. According to these comparisons, T_0 can be used as the standard trackbed model in the following numerical analysis.

4.2 Analysis of vertical acceleration

From the Fig. 6, the range of peak values of the vertical acceleration for T_1–T_4 are about ± 28, ± 22, ± 24, ± 23 m/s^2, which means that the models T_2 and T_4 have smaller vertical acceleration compared to the other two models. Compared to T_4, the acceleration attenuation of T_2 is relatively smaller, which indicates that the asphalt layer located at the lower position of railway trackbed provides higher strength to the structure than that located at the

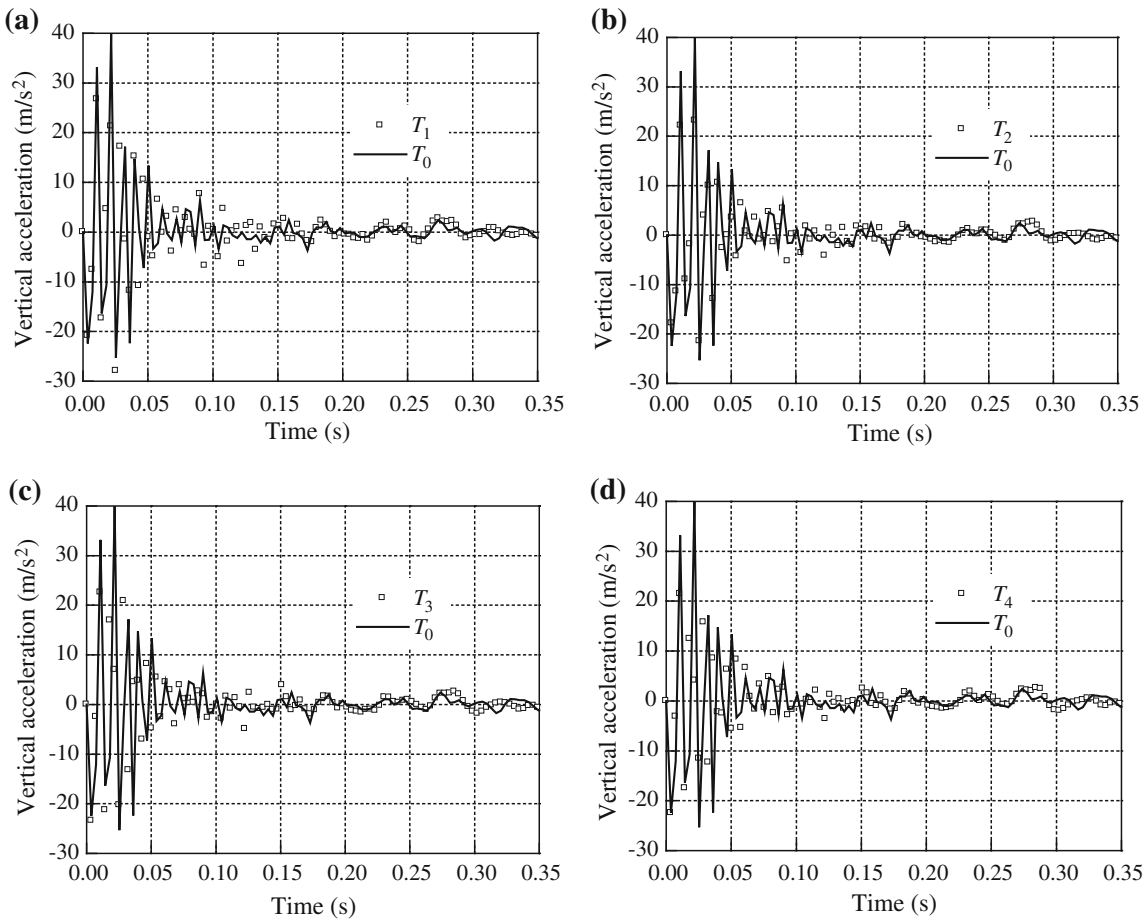

Fig. 6 Time-history curves of vertical acceleration compared to T_0. **a** T_1 versus T_0, **b** T_2 versus T_0, **c** T_3 versus T_0, **d** T_4 versus T_0

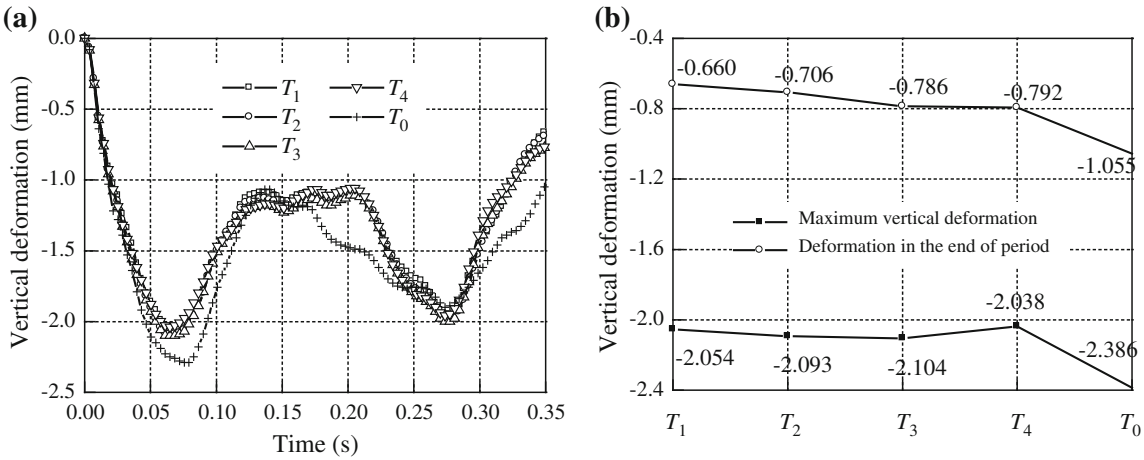

Fig. 7 Comparison of vertical deformation results. **a** Time-history curves **b** Maximum values comparison

upper position. In summary, the asphalt layer can greatly decrease the vertical acceleration at the top of subgrade. This also indicates that the asphalt layer is beneficial to long-term performance and vibration control.

4.3 Analysis of vertical deformation

The time-history curves of vertical deformation at the top of subgrade surface are extracted to compare the maximum value as shown in Fig. 7a, b.

Compared to T_0, the peak values of vertical deformation were decreased from around 2.39 to 2.04–2.10 mm, i.e., 12–15 % decrease. When approaching the end of calculation, the vertical deformation was decreased from about 1.06 to 0.66–0.79 mm, i.e., nearly 25–37 % decrease. This indicates that the four trackbeds with asphalt layer could decrease the maximum vertical deformation at subgrade surface, and the deformation of T_3 was slightly greater than the other three structures. During the calculation period, the maximum vertical deformations of T_1, T_2, T_3, and T_4 were 2.055, 2.049, 2.105 mm (max), and 2.038 mm, respectively. At the end of the calculation, the vertical deformations were 0.661, 0.706, 0.786, and 0.792 mm (max), which shows that T_1 and T_2 are more appropriate for railway asphalt trackbeds than the other two in terms of vertical deformation.

4.4 Analysis of horizontal strain at the bottom of asphalt layer

The horizontal strains include the ones both in transversal and longitudinal directions. The horizontal strain (tensile strain actually) should be less than the allowable tensile strain of asphalt mix. In this calculation, the time-history curves of transversal and longitudinal strains on the bottom of asphalt layer of four asphalt trackbed models were extracted and then compared to the horizontal strain as shown as Fig. 8.

The longitudinal tensile strain obtained for section T_4 was 4.136 με, which is the minimum among the four structures. The time-history curve of T_4 (Fig. 8a) shows that the strain was mainly a compressive strain. However, the maximum transversal tensile strain was about 61.222 με, which was almost twice than the corresponding values of other three structures. This reveals that the trackbed with asphalt layer at the top of ballast trackbed mainly experiences transversal tensile stress while being compressed in longitudinal direction, which is similar to being in the state of simple tensile stress and is adverse to the long-term performance of asphalt layer.

For the model T_1, the maximum transversal and longitudinal tensile strains at the bottom of asphalt layer were about 32.438 and 33.896 με, respectively, which were 15 % and 33 % greater than those of T_2 and also 7 % and 47 % greater than T_3. Based on the time-history curves (Fig. 8b), the horizontal strains of T_1 (especially the longitudinal) were greater than both T_2 and T_3 structures. This indicated that the inner stress of the asphalt layer in T_1 is more concentrated than T_2 and T_3, which is not beneficial to the long-term performance for asphalt material. As shown in Fig. 8b, the time-history curves of T_2 and T_3 were similar and the maximum values were 27.543 and 30.975 με, relatively smaller than those of the other two structures, while the maximum longitudinal strain of T_2 was about 22 % greater than the other structures. The time-history curve of T_2 is flatter than that of T_3, which indicates that the usage of asphalt mix in T_2 can result in better mechanical performance of asphalt mix both in transversal and longitudinal direction. Thus, T_2 and T_3 structures were more appropriate for asphalt railway trackbeds than T_1 and T_4, and the horizontal strain of T_2 was slightly less than T_1.

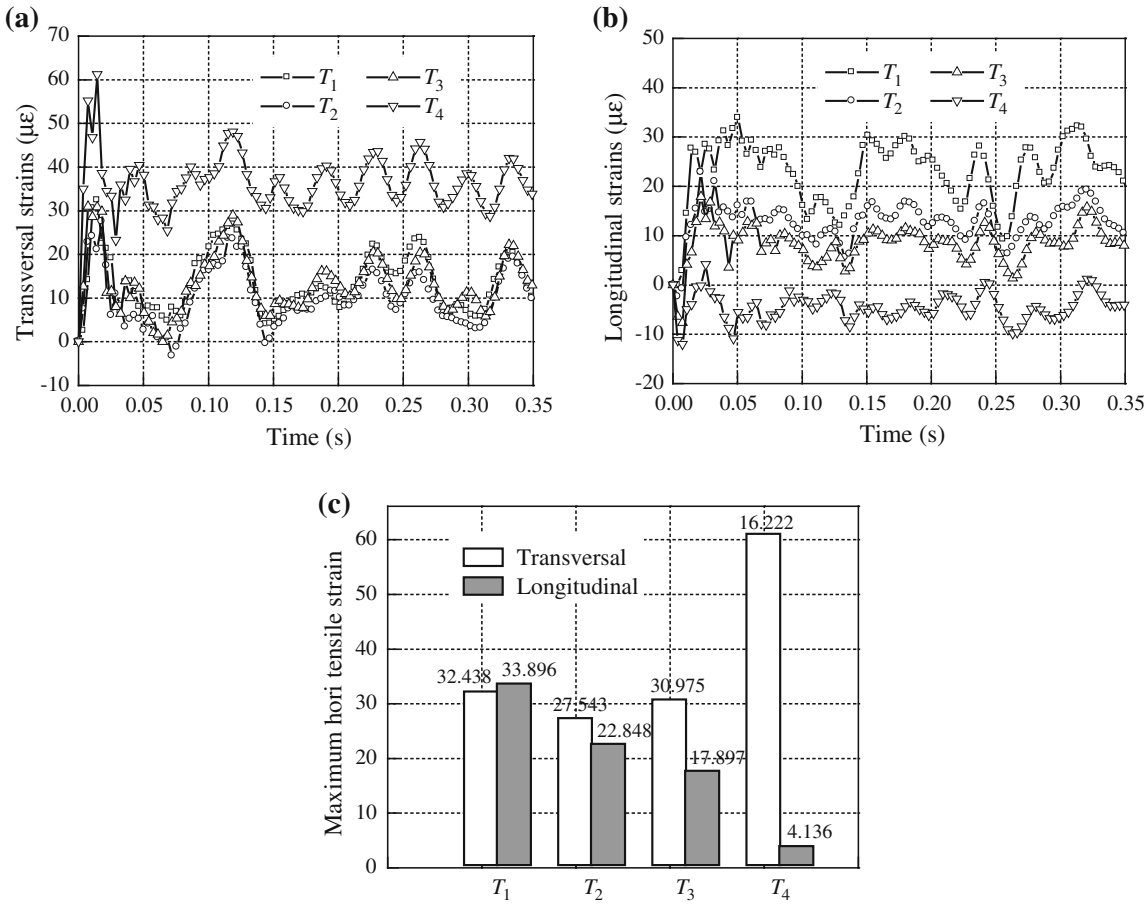

Fig. 8 Horizontal strains on the bottom of asphalt layer. **a** Time-history curves of trans. strains **b** Time-history curves of long. strains **c** Maximum hori. tensile strain

4.5 Comprehensive evaluation of four asphalt trackbeds

From the above, the four asphalt railway trackbeds are evaluated as shown in Tables 2 and 3, where the mark "$\surd$" means that the value meets the requirement of the specific parameter, and the mark "$\times$" means that the value does not. According to Tables 2, 3, the structure T_2 with the asphalt mix at the upper of subgrade surface layer is the optimal for railway asphalt trackbeds.

5 Conclusions and suggestions

Four FEM models of asphalt railway trackbeds, T_1, T_2, T_3, and T_4, were established using ABAQUS and compared with the conventional ballasted railway trackbed model T_0. The main conclusions and suggestions are summarized as follows:

(1) The usage of asphalt layer is beneficial to long-term performance of high-speed trakcbeds especially for the vibration control. The asphalt layer located at the lower part of trackbed provides more vibration attenuation than the upper location, because the range of peak vertical accelerations on the top of subgrade surface of T_2 and T_4 were smaller than T_1 and T_3.

(2) Asphalt layer has the capacity to decrease the maximum vertical deformation of subgrade compared to the conventional ballasted structure, and T_1 and T_2 are more appropriate for railway asphalt trackbeds than T_3 and T_4.

(3) The longitudinal tensile strain of T_4 is the minimum among the four structures; however, the maximum transversal tensile strain of T_4 is almost twice than the other three. The maximum horizontal tensile strain of T_1 was greater than those of T_2 and T_3.

(4) When the asphalt layer is located at the lower part of railway trackbed, the trackbed bears more stress than the case of the asphalt layer at the upper position. The asphalt layer on the upper subgrade (T_2) is proved to be the optimal location of railway asphalt layer.

Acknowledgments This research was supported by the Fundamental Research Funds for the Central University (WUT:2013-IV-067) and National Natural Science Foundation of China (NSFC:50978222).

References

1. Momoya Y (2007) New Railway Roadbed Design. Railw Technol Avalanche 20:118
2. Momoya Y, Sekine E (2007) Performance-based design method for railway asphalt roadbed [J]. RTRI Rep 63(4):608–619
3. Teixeira P, López-Pita A, Casas C et al. Improvements in high-speed ballasted track design benefits of bituminous subballast layers. Transp Res Rec J Transp Res Board No. 1943, Transportation Research Board of the National Academies, Washington, D.C., 2006:43–49
4. Huurman M, Markine V, Man A (2002) Design calculations for embedded rail in asphalt. Proceedings of Railway Engineering 2002 Conference, London, UK, 3–4 July 2002
5. Rose J, Teixeira P, Veit P (2011) International design practices, applications, and performances of asphalt/bituminous railway trackbeds. GEORAIL 2011—International symposium, Paris, France, 19–20 May 2011
6. Rose J, Su B, Long W (2003) Kentrack: a structural analysis program for heavy axle load railway trackbed designs. Proceedings of the international conference and exhibition railway engineering 2003, London, UK, 30 April–1 May 2003—CDROM
7. He H (2005) China's high-speed railway lines need to develop ballastless track. Chin Railw 1:11–15
8. Lei X (2008) Numerical analysis method of railway track structure. China Railway Press, Beijing
9. Ministry of Railway. The provisional design specification for new construction with speed of 200–250 km/h for China's High-speed Railway. TJS[2005] No. 140, China Railway Press, Beijing
10. Fang M (2012) Structural behavior and mix design for asphalt concrete substructures in high-speed rail. Ph.D. Dissertation, Southwest Jiaotong University, Chengdu
11. Li Y, Metcal F (2005) Two-step approach to prediction of asphalt concrete modulus from two-phase micromechanical models. Mater Civ Eng 17(4):407–415
12. Rose J, Su B (2004) Comparisons of railroad track and substructure computer model predictive stress values and in-situ stress measurements. Proceedings of the AREMA 2004 Annual Conference & Exposition, Nashville, TN, September
13. Huang Y. Pavement Analysis and Design [M]. *Pearson Prentice Hall Inc*., Second Edition, 2004
14. Jenkins HH, Stephenson JE, Clayton GA et al (1974) The effect of track and vehicle parameters on wheel/rail vertical dynamic forces. Railw Eng J 3(1):2–16
15. Xu J, Tong X, Pan W (2006) Dynamic FEM Study on Subgrade Structure of High-Speed Rails. Subgrade Eng 5:20–22
16. Su Q, Cai Y (2000) Deformation analysis on subgrade structure of high-speed rails. Subgrade Eng 1:1–3
17. Sun C, Liang B, Yang Q (2003) Test and analysis for the dynamic stress responses of the qin-shen railways subgrade. J Lanzhou Railw Univ (Nat Sci) 22(4):110–112